2301-9069 (e)
1829-8370 (p)

Kapal: Jurnal Ilmu Pengetahuan dan Teknologi Kelautan
(Kapal: Journal of Marine Science and Technology)

journal homepage : http://ejournal.undip.ac.id/index.php/kapal

Assessment of Aerodynamic Performance of Darrieus H-Rotor Wind Turbine Using Realizable k−ε Turbulence Model Approach

Rizki Mendung Ariefianto[1)*)], Elyas Nur Fridayana[2)] , Wisnu Wardhana[2)]

[1)] Department of Electrical Engineering, Faculty of Engineering, Brawijaya University, Malang 65145, Indonesia
[2)] Department of Ocean Engineering, Institut Teknologi Sepuluh Nopember, Surabaya 60111, Indonesia
[*)] Corresponding Author : rizki.mendung.a@ub.ac.id

Article Info

Keywords:
Aerodynamics;
Darrieus H-Rotor;
CFD Simulation;
Turbulence Model k − ε ;
Wind Turbine;

Article history:
Received: 29/07/2024
Last revised: 31/08/2024
Accepted: 03/09/2024
Available online: 31/10/2024
Published: 31/10/2024

DOI:
https://doi.org/10.14710/kapal.v20i3.65458

Abstract

Wind energy extraction gains more attractiveness as the development of renewable energy progresses and the reduction of fossil fuel usage becomes imperative. Consequently, numerous efforts have been made to enhance turbine performance, such as with the Darrieus H-Rotor type, through numerical studies such as Computational Fluid Dynamics (CFD), which underpins turbulence models. This research evaluates the performance of the Darrieus H-Rotor Wind Turbine via 2D CFD modeling using the Realizable k−ε turbulence model. The study also considers simulations with the Double Multiple Streamtube (DMST) model and other turbulence models applied to similar turbine geometries, with experimental data serving as validation benchmarks. Approximately 140,000 cells were utilized in the meshing process to balance simulation duration and the accuracy of the C_p value. The results indicate that the Realizable k−ε turbulence model performs satisfactorily, particularly in producing accurate C_p values in the pre-stall region. The comparison of average C_p values against experimental data across eight tip speed ratio points further supports the effectiveness of the Realizable k−ε turbulence model in simulating the aerodynamic performance of the Darrieus H-Rotor Wind Turbine. Nonetheless, the Realizable k−ε turbulence model fails to enable the Darrieus H-Rotor Wind Turbine to achieve positive C_m values across the entire azimuthal angle at lower tip speed ratios, thus not reaching effective self-starting conditions. In general, the use of CFD-based methods provides results that are closer to experimental values compared to simpler methods without considering turbulence aspect, such as DMST, which tend to produce higher C_p deviations.

1. Introduction

The high dependence on fossil energy encourages humans to look for more abundant renewable energy sources while being able to mitigate problems such as environmental pollution [1] and the greenhouse effect [2]. One of the most popular renewable energies is wind energy because it is clean and easily accessible [3]. To extract wind energy effectively, wind turbines were introduced as a reliable conversion tools. In general, wind turbines are categorized based on their axis into horizontal axis wind turbines (HAWT) and vertical axis wind turbines (VAWT). Although HAWT have the advantage of high efficiency, VAWT offer other advantages such as their simple structure, ability to convert omnidirectional wind, minimal noise, stability under turbulence conditions, integration with other structures, and easy placement of generators, gearboxes, and bearings [4], [5], [6]. In practice, there are two well-known VAWT turbines, namely the Savonius type, which utilizes drag force, and the Darrieus type, which utilizes lift force [7]. Both forces are greatly influenced by the aerodynamic performance of a wind turbine. Hence, the airfoil design applied to the turbine blades must be designed as well as possible in order to obtain optimal aerodynamic performance. An airfoil is a special geometric shape designed to increase lift (increased lift coefficient) and reduce drag (reduced drag coefficient) [8]. In fluid dynamics, airfoil lift occurs due to the pressure difference between the upper and lower surfaces caused by the angle of attack (AoA) and the influence of the camber shape of the airfoil.

Conventionally, the aerodynamic performance of wind turbines has been estimated using the blade element momentum (BEM) theory, which exhibits beneficial aspects such as its simplicity and fast computation [6]. However, this method is limited by the lack of airfoil databases and aerodynamic coefficients for the airfoils used [9]. Most existing airfoil databases are modified from aviation applications, which are not fully suitable for describing wind turbine blade aerodynamics. These aviation-based airfoil designs generally work at relatively high Reynolds numbers (above Re = 10^6), whereas wind turbines typically operate at lower Reynolds numbers (close to Re = 10^5). The airfoil data requirements for VAWT applications are actually broader than for the aviation industry. This occures because VAWTs require analysis down to the small details of the blade profile and consider energy extraction processes where the basic structure of the flow field inside the rotor volume cannot be visualized using classical computational methods [10].

The limitation of accurate aerodynamic data at low Reynolds numbers can be overcome by using Computational Fluid Dynamics (CFD) codes that have accurate performance in predicting wind turbine models [11]. CFD can also clarify the physical phenomena underlying the unstable power conversion of turbines and characterize the aerodynamic performance under the influence of various geometry parameters [12]. A widely used CFD method for wind turbine model computations is the Reynolds-Averaged Navier-Stokes (RANS). The essence of RANS modeling is to mathematically resolve the complexities of the Reynolds stress problem. A common method to address the issue is by using the Boussinesq hypothesis-based eddy viscosity, which assumes a linear relationship between the Reynolds stress and the local average strain rate tensor [13]. This approach serves to model the varying flow and is closely related to turbulence models, some of which are known, including Spalart-Allmaras, k-ω, and k-ε [14].

Several studies have explored the application of these turbulence models to VAWT simulations. Authors in [15] conducted a comparison of turbulence models applied to Savonius-type wind turbines. Based on two-dimensional simulations, the Realizable k-ε turbulence model was found to be a suitable model for predicting the static torque characteristics of this turbine when compared to the k-ω and Spalart-Allmaras turbulence models. A more complex comparison of these turbulence models was conducted by [16]. A total of six turbulence models were compared in this study. In its application to Darrieus wind turbines, it was found that the Realizable k-ε turbulence model gave the closest results to experimental data compared to other turbulence models such as Spalart-Allmaras, SST Transition, SST k-ω, RNG k-ε, and υ2-f. In [17], a Darrieus H-Rotor Wind Turbine was investigated using 2D CFD modeling. The result is that the application of the Realizable k-ε turbulence model has good validation of experimental data. Research using the same turbine type and simulation model was also conducted by [18]. The results of using the Realizable k-ε turbulence model show acceptable calculations and are quite close to the validation reference experimental results.

Based on previous research, the Realizable k-ε turbulence model is quite effective for predicting VAWT performance. Therefore, in this study, numerical modeling of the Darrieus H-Rotor Wind Turbine based on the Realizable k-ε turbulence flow model is carried out using CFD simulation. The results are compared with other methods such as DMST, with accuracy measured against experimental test results of similar Darrieus H-Rotor Wind Turbines. To reduce complexity and simulation time, this study considers solving the simulation in the 2D domain. The output of this research can be used as a reference for the use of simulation methods in modeling turbines, allowing for an evaluation of how well the model represents actual physical phenomena.

2. Methods

2.1. Geometric and Boundary Design

In this study, the Darrieus H-Rotor Wind Turbine model used as a reference is sourced from the research of [10] as shown in Figure 1. This turbine has three blades with an airfoil profile using the NACA 0021 type with the geometry shown in Table 1. This airfoil is chosen because it has availability of experimental data as conducted by [10]. Technically, NACA 0021 has been used in many turbine modelings because it offers good performance at low TSR [19] and efficiency in order to increase the blade works [20]. This turbine is a development of a straight blade Darrieus turbine whose radius connection is located at the tip of the blade. The domain boundary is defined as a semicircular shape near the inlet. This aims to reduce the meshing area that is unnecessary in the region close to the inlet. Specifically, the simulation domain boundaries consist of several parts as shown in Figure 2. The outer boundaries include the red line representing the inlet, the green line representing the outlet, and the black line representing symmetry. The inner boundaries include the blue line as the rotary zone, the light blue line as the stationary zone, the orange line as the blade zone rotating with the rotary zone, and the purple area representing the airfoil. The total length of the domain is 17 times the radius (R), with a distance of $5R$ from the inlet to the turbine shaft and $12R$ from the outlet to the turbine shaft. The geometric data and boundary condition definitions are subsequently applied using ANSYS software, with results shown in Figure 3.

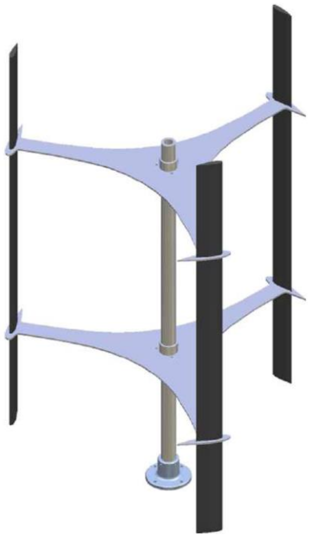

Figure 1. The design construction of Darrieus H-Rotor Wind Turbine from [10]

Table 1. The geometric properties of the Darrieus H-Rotor Wind Turbine

Geometric Parameters	Notation	Value
Airfoil	-	NACA 0021
Number of blades	N	3
Turbine height	H	1.457 m
Turbine diameter	D	1.030 m
Chord length	c	0.0858 m
Solidity	σ	0.5
Turbine sweep area	A	1.236 m^2

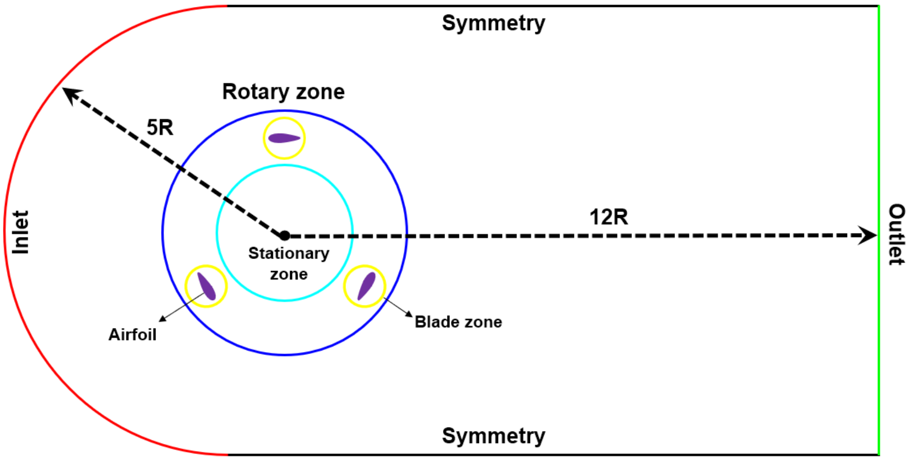

Figure 2. Setting boundary conditions in the simulation

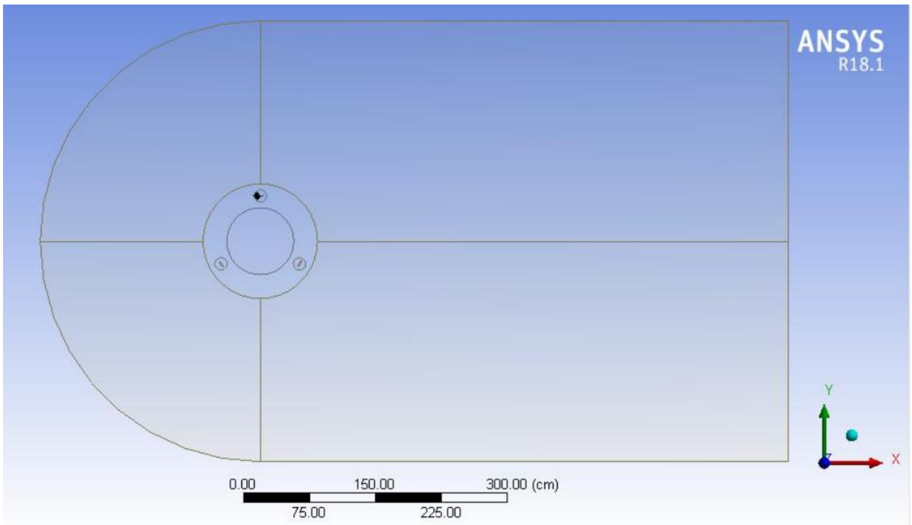

Figure 3. Application of geometry and domains in ANSYS

2.2. Meshing Process

Meshing is a critical component of CFD simulation design that can determine the final outcome of the numerical study. Using a greater number of finer mesh elements yields better final results. However, a higher number of fine mesh elements also demands longer simulation times. Therefore, a meshing strategy that employs fine elements while reducing simulation duration is required. In this simulation, a quadrilateral mesh profile with an unstructured mesh type is considered.

The meshing structure strategy involves increasing the number of meshes in more critical areas. As shown in Figure 4, the meshing implementation results in an increased number of meshes in the rotary zone, slightly reduced in the inlet region, and further reduced towards the outlet. The meshing process in the rotary zone also has gradations, where the region closest to the airfoil is much finer and denser compared to the blade zone and the stationary zone, as illustrated in Figure 5 (a-d).

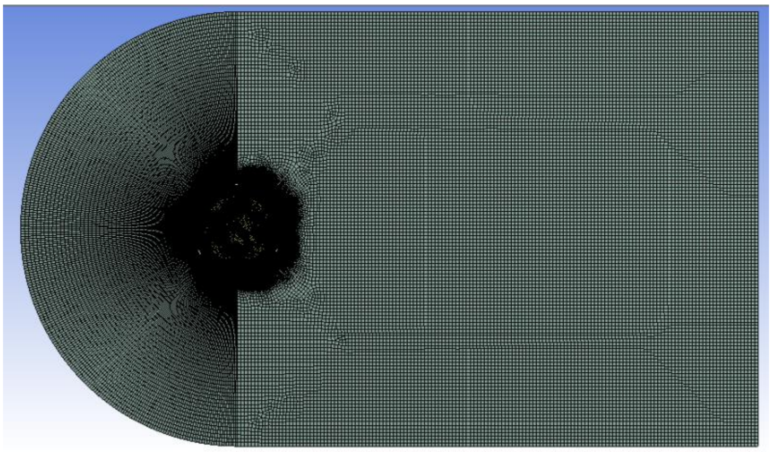

Figure 4. Meshing result for whole domain

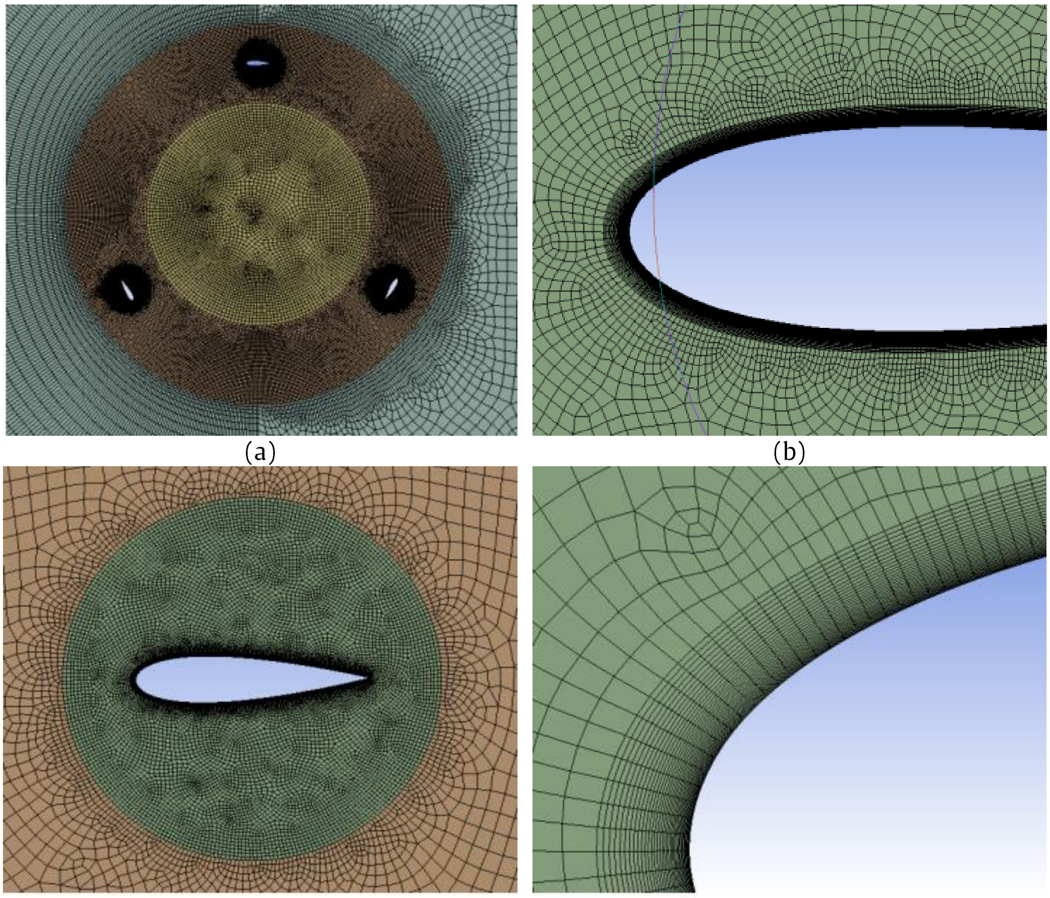

(a) (b)

(c) (d)

Figure 5. Meshing result for (a) rotary zone, (b) blade zone, (c) airfoil zone, and (d) airfoil surface

2.3. Advance Consideration in Simulation Process

The determination of simulation support parameters significantly influences the results. Therefore, several factors were considered in conducting this simulation. The freestream wind speed was kept constant at 9 m/s with a uniform flow direction, under transient and incompressible conditions. The air properties used include a density of 1.225 kg/m³ and a dynamic viscosity of 1.7894 x 10^{-5} kg/ms. The calculation process was performed at every 2° rotation of the rotor, with a total rotation of three complete turns (1080°). The moment coefficient (C_m) considered was derived from the overall moment value at each final rotation or every 360°. This approach was taken to achieve stable results under steady-state conditions. The sliding mesh technique was employed to model the rotating turbine.

The 2D simulation of the Darrieus H-Rotor turbine was conducted under transient flow conditions. The computations aimed to resolve incompressible turbulence using the unsteady Reynolds Averaged Navier-Stokes (U-RANS) equations. Additionally, the application of a turbulence model, specifically the eddy viscosity type, was considered to achieve more accurate results. The turbulence model selected was the Realizable k−ε model, which previous research has shown to be effective in assessing VAWT performance. This CFD code was also compared with other CFD studies investigating the same turbine geometry and other computational models such as DMST. The obtained results were validated for accuracy by referencing the experiments conducted by [10].

In the simulation's residual monitor settings, iteration values were adjusted to ensure convergence. Iterations were deemed convergent when the residual value was less than the maximum allowable error. Once convergence was achieved, the iterations ended, and computation proceeded to the next time step. Therefore, in this simulation, convergence was set with an overall equation tolerance of 10^{-4} and a maximum of 80 iterations. The number of time steps (NTS) was designed so that the blade traveled 2°, calculated as follows [21]:

$$NTS = n \times \frac{360°}{\Delta\theta} \quad (1)$$

n and $\Delta\theta$ are the desired number of revolutions and increment angle, respectively. After obtaining the NTS, the time step size (TSS) can be calculated with the following equation:

$$TSS = \frac{2\pi n}{\omega \times NTS} = \frac{2\pi\Delta\theta}{\omega \times 360°} \quad (2)$$

ω is the angular velocity of the turbine (rad/s).

2.4. Key Parameters of VAWT Performance

Several performance parameters for VAWTs are defined to aid in the completion of the simulation analysis. The key parameters considered begin with the turbine power equation (P_t) as follows:

$$P_t = C_p P_a = C_p \frac{1}{2} \rho A_t v^3 \quad (3)$$

where C_p is the turbine power coefficient, ρ is the air density (kg/m³), A_t is the turbine swept area (m²), and v is the wind speed (m/s). The value of C_p is given by:

$$C_p = \lambda C_m \quad (4)$$

where C_m is the blade moment coefficient (obtained from the simulation) and λ is defined as the tip speed ratio (TSR), which has the following equation:

$$\lambda = \frac{\omega R}{U_\infty} \quad (5)$$

Here, R is the turbine radius (m), and ω is the angular velocity (rad/s). The Reynolds number (Re) can be determined using the following equation:

$$Re = \frac{\rho v c}{\mu} \quad (6)$$

where c is the chord length of the foil, and μ is the dynamic viscosity of the air (kg/ms).

3. Results and Discussion

3.1. Sensitivity Mesh Analysis

In CFD simulations, the meshing strategy is very crucial. Hence, a mesh sensitivity study was conducted to determine the optimal meshing strategy. To strike a compromise between computational time and accuracy, different mesh counts were tried. Initially, a mesh size of 80,000 cells was selected and increased to 170,000 cells in increments of 30,000 cells. A mesh size of 80,000 cells is considered the minimum mesh size, as used in many vertical axis studies such as those by [22], [23]. This test was applied at a λ value of 3.3. Based on the mesh sensitivity test results, as shown in Figure 6, the C_p value consistently decreased until it reached 170,000 cells, which indicates a more accurate result. However, when it reaches a mesh count of 140,000 cells, the addition of the next mesh does not really give significant results. This is shown by the percentage difference at mesh counts of 140,000 and 170,000, which is only 0.24%. Therefore, a mesh count of 140,000 cells was selected in this study. The use of this mesh number of 140,000 cells in one simulation takes 660 minutes (11 hours) with standard computer capabilities (dual-core CPU). Authors in [24] recommended that a mesh size of 140,000 is a good consideration for simulating turbulence models, as performed in this study. This mesh count was also used in VAWT studies by [25] and [26].

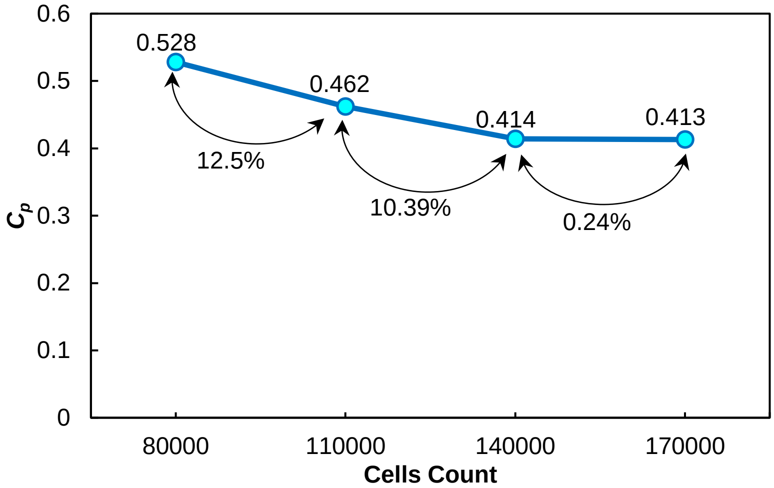

Figure 6. Sensitivity mest test results for C_p value

3.2. Analysis of Coefficient of Blade Moments

In this section, the coefficient of blade moment (C_m) is the output of the simulation. This coefficient is then plotted against the azimuthal angle during the inputing rotation period. This C_m value will later be used to obtain the coefficient of power (C_p). The C_m value considered is the average value in the third rotation or in the angle range of 720° to 1080°. This is done to obtain a representative C_m value because it has reached a steady state condition. There are eight C_m values reviewed according to the number of tip speed ratios in the research of [10]. The tip speed ratio values are shown in Table 2.

Table 2. The value of λ reviewed in the simulation

λ	ω (rad/s)
1.44	25.165
1.70	29.709
2.05	35.825
2.33	40.718
2.52	44.039
2.60	45.437
3.10	54.175
3.30	57.670

This study also considers the results of other DMST-based methods used as a comparison. DMST model simulation is done first by inputting the considered airfoil and Reynolds number. The Reynolds number value can be calculated as follows:

$$Re = \frac{\rho v c}{\mu} = \frac{1.225 \times 9 \times 0.0858}{1.7894 \times 10^{-5}} \approx 53.000$$

From the simulation results, at one value of λ = 1.7, it is possible to compare the C_m values along the azimuthal angle between CFD using the Realizable k-ε model and DMST as shown in Figure 7 (a). It is evident that the C_m value in the Realizable k−ε CFD model is higher than that in the DMST across all azimuthal angles, with a maximum difference of 0.06. Additionally, the C_m curve produced by the Realizable k−ε CFD model is smoother or less of ripples, indicating that at the same tip speed ratio, the Darrieus H-Rotor Wind Turbine from the Realizable k−ε CFD simulation yields a smoother rotation compared to the DMST method. However, the Realizable k−ε CFD simulation generates a larger negative torque than DMST, indicating that the Darrieus H-Rotor turbine has not yet achieved self-starting capability. In the overall simulation, DMST does not actually show positive C_m values throughout the azimuthal angles at all tip speed ratio. This highlights one of the weaknesses of the DMST method, as it fails to adequately simulate certain physical phenomena.

In contrast, the Realizable k−ε CFD simulation achieves positive torque at all azimuthal angles when λ = 2.52, as shown in Figure 7 (b). It can be seen that the Realizable k-ε method results in smoother rotation compared to its previous state at λ = 1.7, indicated by a complete reduction in ripple along the azimuthal angle. At this λ value, the torque also increases significantly. The DMST method also shows positive regimes for C_m, although the ripples tend to increase compared to its previous state at λ = 1.7. Nevertheless, according to research of [27], Darrieus turbines typically achieve self-starting at $\lambda \geq$ 2. Thus, a Darrieus H-Rotor Wind Turbine design that achieves self-starting at λ = 2.52 requires modification to enhance performance, as suggested by [28]. This analysis remains incomplete, as it is limited to 2D simulations; therefore, the impact of physical variables can be more comprehensively covered in 3D simulations. Overall, the C_m characteristics in the CFD simulation are superior to those in the DMST, particularly at low tip speed ratios, as confirmed by [29].

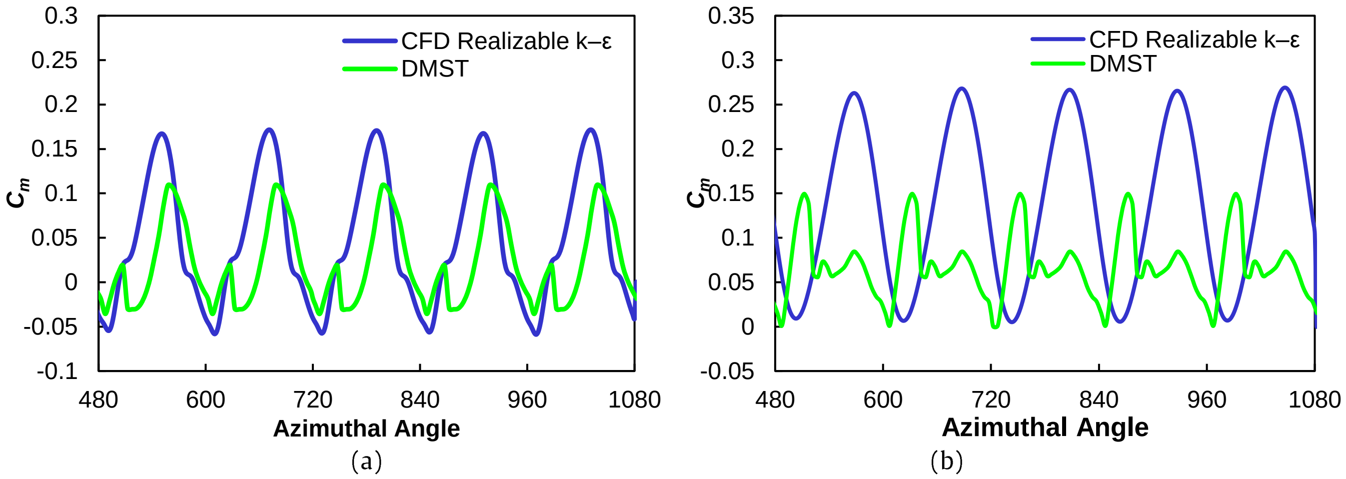

Figure 7. C_m result between CFD Realizable k−ε and DMST at (a) λ = 1.7 and (b) λ = 2.52

3.3. Comparison of Coefficient of Power Under Different Model

The average moment coefficient (C_m) multiplied by the tip speed ratio (λ) yields the turbine power coefficient (C_p). With identical geometric variables, the C_p values from the Realizable k−ε CFD simulation can be compared to those from similar studies, particularly in 2D simulations. Studies considered include those by Sobhani et al [30], Celik & Kaya [31], and Ni et al [32], as well as validation references from Castelli et al [10]. The C_p values compared in each study are extracted from graphs corresponding to the eight specified λ values. The results are shown in Figure 8 indicate that all studies exhibit similar characteristics to the experiments, with the C_p values consistently increasing in the pre-stall region from λ = 1.44 to λ = 2.52. In the comparison of the same turbulence model, Realizable k−ε, the current study shows better results at all tip speed ratios compared to the studies by [10] and [31], which over-predicted the C_p values. When compared to the Transition SST turbulence model, the current study consistently aligns more closely with the experimental results. Additionally, the Realizable k−ε model in this study competes favorably with the SST k−ω model used by [30] and [32], particularly in the pre-stall region. Notably, the experimental results were closely matched at two tip speed ratio points, λ = 2.05 and λ = 2.33. This advantage is further highlighted in Figure 9, where the current study exhibits the lowest average C_p deviation from experimental results, indicating high accuracy. Interestingly, the present study using Realizable k-ε obtains a similar C_p different compared with [30], which used the SST k−ω model. With the same turbine geometries, this may be possible if the boundary layer characteristics around the turbine blades are also similar.

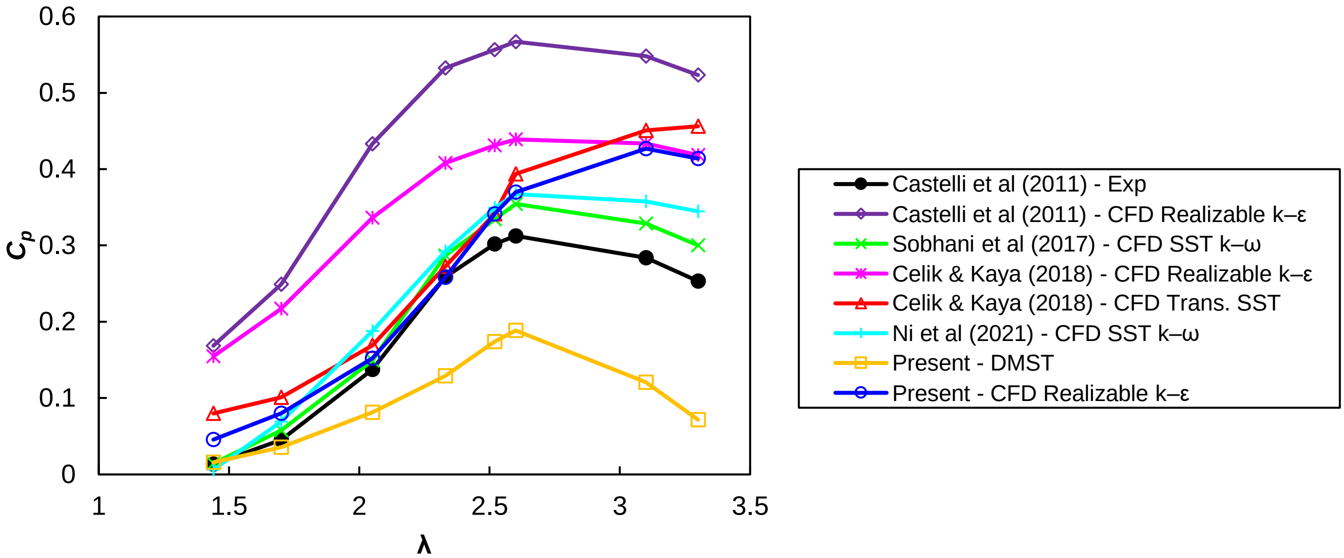

Figure 8. Comparison of C_p values from other research and present study

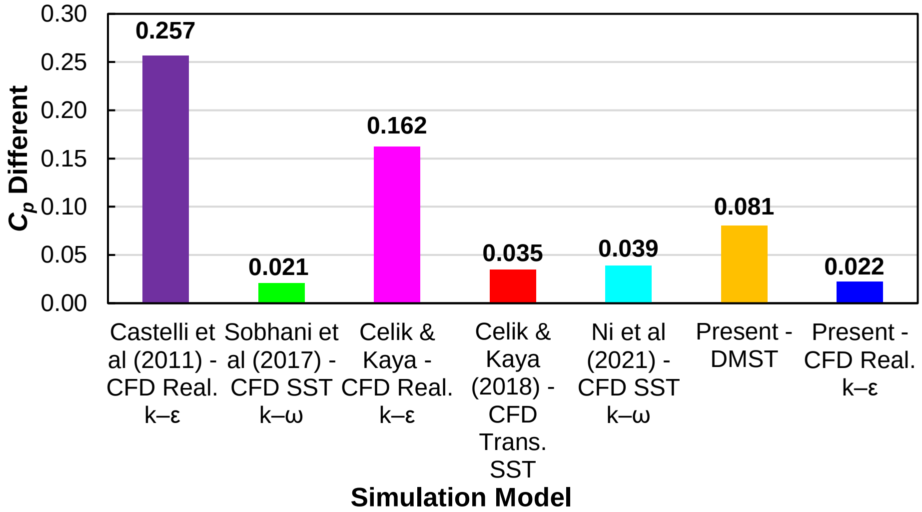

Figure 9. C_p values different from all simulation models

However, when the turbine reaches stall at $\lambda \geq 2.6$, the C_p values tend to be significantly higher than the experimental results due to the limitations of numerical studies in modeling the flow around the turbine [30]. This includes the current CFD model, which shows a stall point that is quite distant from the experimental results, leading to a large deviation in C_p values. On the other hand, the DMST trend aligns with experimental results up to the stall point, even though the C_p values are quite far off, leading to a significant difference in C_p and under-prediction of C_p. The DMST method is significantly influenced by local Reynolds numbers; lower Reynolds numbers result in lower C_p values [33]. Furthermore, the magnitude of C_p is heavily dependent on the extrapolation of coefficients using methods like Montgomerie or Viterna, which lack universally applicable objective standards. In addition, the DMST method is a simple approach for calculating blade behavior without considering more complex aspects, such as turbulence, which are addressed in CFD methods.

Ultimately, it is found that all CFD simulations based on turbulence models yield C_p values higher than experimental results. This discrepancy arises from the use of 2D CFD models, which do not account for phenomena such as tip vortices and flow divergence [34]. These factors can cause tip losses, impacting the obtained C_p values. Moreover, in 2D modeling, singularities can easily arise between adjacent segments. Singularities are evident at maximum thickness due to rotation and can cause discontinuities in the blade curvature surface, affecting aerodynamic performance [35]. The DMST model also encounters similar issues in flow modeling around the blades and convergence problems in airfoil simulations [6]. Moving to 3D simulations offers a promising advancement as they can capture more detailed physical phenomena. For example, the impact of singularities can be addressed through the distribution of source and sink elements on panels, not only between adjacent panels but also across other panels.

4. Conclusion

In this study, the Darrieus H-Rotor Wind Turbine has been validated through 2D CFD modeling using the Realizable k–ε turbulence model. This model has proven capable of accurately representing the turbine's characteristics, closely aligning with experimental C_p data. Comparative analysis against studies assuming similar turbine geometry and other CFD models, as well as the DMST model, indicates that the Realizable k–ε turbulence model performs satisfactorily, particularly in the pre-stall region. This same turbulence model can certainly be applied to 3D simulations to address physical phenomena such as flow divergence, tip vortices, and singularities, which are not accounted for in 2D simulations. However, the Realizable k–ε turbulence model still does not enable the Darrieus H-Rotor Wind Turbine to achieve positive C_m values throughout the azimuthal angle at lower tip speed ratios, thus failing to attain effective self-starting conditions. Consequently, physical modifications to the turbine are also necessary to comprehensively enhance its performance. This finding can serve as a good recommendation for developing the initial design of a vertical axis turbine. In the next study, it is recommended to conduct 3D simulations that consider more detailed aspects to obtain more accurate results of turbine performance.

References

[1] R. M. Ariefianto and R. A. Aprilianto, "Peluang Dan Tantangan Menuju Net Zero Emission (NZE) Menggunakan Variable Renewable Energy (VRE) Pada Sistem Ketenagalistrikan Di Indonesia," *Jurnal Paradigma: Jurnal Multidisipliner Mahasiswa Pascasarjana Indonesia*, vol. 2, no. 2, pp. 1–13, 2021.

[2] R. M. Ariefianto, R. A. Aprilianto, H. Suryoatmojo, and S. Suwito, "Design and Implementation of Z-Source Inverter by Simple Boost Control Technique for Laboratory Scale Micro-Hydro Power Plant Application," *Jurnal Teknik Elektro*, vol. 13, no. 2, pp. 62–70, 2021.

[3] B. Zouzou, I. Dobrev, F. Massouh, and R. Dizene, "Experimental and numerical analysis of a novel Darrieus rotor with variable pitch mechanism at low TSR," *Energy*, vol. 186, 2019.

[4] M. Ahmadi-Baloutaki, R. Carriveau, and D. S. K. Ting, "Straight-bladed vertical axis wind turbine rotor design guide based on aerodynamic performance and loading analysis," *Proceedings of the Institution of Mechanical Engineers, Part A: Journal of Power and Energy*, vol. 228, no. 7, pp. 742–759, 2014.

[5] S. Y. Cho, S. K. Choi, J. G. Kim, and C. H. Cho, "An experimental study of the optimal design parameters of a wind power tower used to improve the performance of vertical axis wind turbines," *Advances in Mechanical Engineering*, vol. 10, no. 9, pp. 1–10, 2018, doi: 10.1177/1687814018799543.

[6] R. M. Ariefianto, R. N. Hasanah, and W. Wijono, "Analisis Turbin Darrieus Tipe V-Shaped Blade Untuk Aplikasi Konverter Energi Arus Laut Menggunakan Software QBlade," *Jurnal Kelautan Nasional*, vol. 17, no. 2, 2022.

[7] H. Eftekhari, A. S. Mahdi Al-Obaidi, and S. Eftekhari, "Aerodynamic Performance of Vertical and Horizontal Axis Wind Turbines: A Comparison Review," *Indonesian Journal of Science and Technology*, vol. 7, no. 1, pp. 65–88, 2022.

[8] T. Srinivasa Rao, T. Mahapatra, and S. Chaitanya Mangavelli, "Enhancement of Lift-Drag characteristics of NACA 0012," *Materials Today: Proceedings*, vol. 5, no. 2, pp. 5328–5337, 2018.

[9] G. Bedon, M. Raciti Castelli, and E. Benini, "Optimization of a Darrieus vertical-axis wind turbine using blade element - momentum theory and evolutionary algorithm," *Renewable Energy*, vol. 59, pp. 184–192, 2013.

[10] M. Raciti Castelli, A. Englaro, and E. Benini, "The Darrieus wind turbine: Proposal for a new performance prediction model based on CFD," *Energy*, vol. 36, no. 8, pp. 4919–4934, 2011.

[11] A. A. Shoukat et al., "Blades optimization for maximum power output of vertical axis wind turbine," *International Journal Renewable Energy Development*, vol. 10, no. 3, pp. 585–595, 202.

[12] A. Rezaeiha, H. Montazeri, and B. Blocken, "Towards accurate CFD simulations of vertical axis wind turbines at different tip speed ratios and solidities: Guidelines for azimuthal increment, domain size and convergence," *Energy Conversion and Management*, vol. 156, pp. 301–316, 2018.

[13] S. D. Hornshøj-Møller, P. D. Nielsen, P. Forooghi, and M. Abkar, "Quantifying structural uncertainties in Reynolds-averaged Navier–Stokes simulations of wind turbine wakes," *Renewable Energy*, vol. 164, pp. 1550–1558, 2021.

[14] Y. Elyas Nur Fridayana, S. Hadiwidodo, and D. Satrio, "Studi Pemilihan Model Turbulen pada Vertical Axis Water Turbine (VAWT) Tipe Gorlov Menggunakan Metode Computational Fluid Dynamics," *Syntax Literate: Jurnal Ilmiah Indonesia*, vol. 7, no. 6, pp. 2003–2005, 2022.

[15] S. Roy and U. K. Saha, "Comparative analysis of turbulence models for flow simulation around a vertical axis wind turbine," in Indo-Danish International Conference on Wind Energy: Materials, Engineering, and Policies (WEMEP 2012), pp. 1–6, 2012.

[16] C. Song, Y. Zheng, Z. Zhao, Y. Zhang, C. Li, and H. Jiang, "Investigation of meshing strategies and turbulence models of computational fluid dynamics simulations of vertical axis wind turbines," *Journal of Renewable and Sustainable Energy*, vol. 7, no. 3, 2015.

[17] I. Hashem and M. H. Mohamed, "Aerodynamic performance enhancements of H-rotor Darrieus wind turbine," *Energy*, vol. 142, pp. 531–545, 2018.

[18] F. Alqurashi and M. H. Mohamed, "Aerodynamic forces affecting the H-rotor darrieus wind turbine," *Modelling and Simulation in Engineering*, vol. 2020, pp. 1–15, 2020.

[19] T. Zhang, Z. Wang, W. Huang, D. Ingham, L. Ma, and M. Pourkashanian, "A numerical study on choosing the best configuration of the blade for vertical axis wind turbines," *Journal of Wind Engineering and Industrial Aerodynamics*, vol. 201, p. 104162, 2020.

[20] R. M. Ariefianto, R. N. Hasanah, W. Wijono, and A. Ridlwan, "Performance Study of a Humpback Whale Fluke Turbine on Foil Shape Variation Based on Double Multiple Streamtube Model," Kapal: Jurnal Ilmu Pengetahuan dan Teknologi Kelautan; vol. 20, no. 3, pp 320–328, 2023.

[21] D. Satrio, I. Ketut Aria Pria Utama, and Mukhtasor, "The influence of time step setting on the CFD simulation result of vertical axis tidal current turbine," *Journal of Mechanical Engineering and Sciences*, vol. 12, no. 1, pp. 3399–3409, 2018.

[22] M. H. Mohamed, "Reduction of the generated aero-acoustics noise of a vertical axis wind turbine using CFD (Computational Fluid Dynamics) techniques," *Energy*, vol. 96, pp. 531–544, 2016.

[23] E. Fatahian, R. Mishra, F. F. Jackson, and H. Fatahian, "Optimization and analysis of self-starting capabilities of vertical axis wind turbine pairs: A CFD-Taguchi approach," *Ocean Engineering*, vol. 302, 2024.

[24] M. Reggio, F. Villalpando, and A. Ilinca, "Assessment of turbulence models for flow simulation around a wind turbine airfoil," *Modelling and Simulation in Engineering*, vol. 2011, no. 1, 2011.

[25] S. Rolland, W. Newton, A. J. Williams, T. N. Croft, D. T. Gethin, and M. Cross, "Simulations technique for the design of a vertical axis wind turbine device with experimental validation," *Applied Energy*, vol. 111, pp. 1195–1203, 2013.

[26] M. Kear, B. Evans, R. Ellis, and S. Rolland, "Computational aerodynamic optimisation of vertical axis wind turbine blades," *Applied Mathematical Modelling*, vol. 40, no. 2, pp. 1038–1051, 2016.

[27] S. Victor and M. Paraschivoiu, "Performance of a Darrieus turbine on the roof of a building," *Transactions of The Canadian Society for Mechanical Engineering*, vol. 42, no. 4, pp. 341–349, 2018.

[28] R. M. Ariefianto, R. N. Hasanah, and W. Wijono, "Unjuk Kerja Performa Turbin Arus Laut Sumbu Vertikal Pada Berbagai Bentuk Sudu Unik," *Rekayasa*, vol. 15, no. 1, pp. 53–63, 2022.

[29] H. Beri and Y. Yao, "Double Multiple Streamtube Model and Numerical Analysis of Vertical Axis Wind Turbine," *Energy and Power Engineering*, vol. 03, no. 03, pp. 262–270, 2011.

[30] E. Sobhani, M. Ghaffari, and M. J. Maghrebi, "Numerical investigation of dimple effects on darrieus VERTICAL axis wind turbine," *Energy*, vol. 133, pp. 231–241, 2017.

[31] Y. Celik and M. N. Kaya, "Numerical Investigation of The Starting Behaviour of H-Type Vertical Axis Wind Turbine with Different Airfoils," in The International Conference on Innovative Engineering Applications, 2018.

[32] L. Ni, W. Miao, C. Li, and Q. Liu, "Impacts of Gurney flap and solidity on the aerodynamic performance of vertical axis wind turbines in array configurations," *Energy*, vol. 215, p. 118915, 2021.

[33] A. Muratoğlu and M. S. Demir, "Numerical Analyses of a Straight Bladed Vertical Axis Darrieus Wind Turbine: Verification of Dms Algorithm and Qblade Code," *European Journal of Technic*, vol. 9, no. 2, pp. 195–208, 2019.

[34] A. Aihara, V. Mendoza, A. Goude, and H. Bernhoff, "Comparison of Three-Dimensional Numerical Methods for Modeling of Strut Effect on the Performance of a Vertical Axis Wind Turbine," Energies, vol. 15, no. 7, 2022.

[35] Y. Wang, H. Tong, H. Sima, J. Wang, J. Sun, and D. Huang, "Experimental study on aerodynamic performance of deformable blade for vertical axis wind turbine," *Energy*, vol. 181, pp. 187–201, 2019.